Design & Fabrication of Small-Scale Desktop Binder Jet 3D Printer Subassemblies

Keval Babu[1], Gregory Cartagena[2], Han He[3], Amardeep Sidhu[4], Alison Yu[5]

[1, 2, 4, 5]Graduate Student, [3]Undergraduate Student
[1, 2, 3, 4, 5]Department of Mechanical Engineering, Massachusetts Institute of Technology

Abstract

Binder Jet 3D printing is an additive manufacturing technique that utilizes a binding agent to form each layer on a powder bed, ultimately producing a complete part. This method is advantageous for manufacturing due to its ability to handle a diverse range of materials while achieving high complexity and density in printed parts. Currently, industrial Binder Jet 3D printers range in price from $100,000 to $1 million, and they require significant space and energy within a manufacturing facility. Many engineers would benefit from a smaller, more energy-efficient binder jetting solution that allows for rapid testing of printed parts before full-scale production or the prototyping of small-scale components.To address this need, our team has developed a small-scale desktop Binder Jet printer subassembly. The primary focus of this design is to minimize cost, reduce print time, and decrease the printer's footprint, all while maintaining the desired complexity and precision of the parts produced. This paper presents the current design and construction of the proposed device, along with key findings to inform future developments.

Keywords: AM, CAD, FDM, 3D Printing, Binder Jet

Introduction

Conventional Binder Jetting involves a four-step process. Initially, loose powder is deposited from a powder bed onto a print bed. Subsequently, a roller compacts and smoothens the powder layer to ensure uniformity. Following this, the print head dispenses a binder (tailored to the specific type of powder) to bind the powder particles together. Lastly, the print bed is lowered while the powder bed is raised, and a new layer of powder is added. This cycle is repeated until the completion of the part, known as a “Green Part.” Figures 1 illustrates the conventional binder jet printing process below.

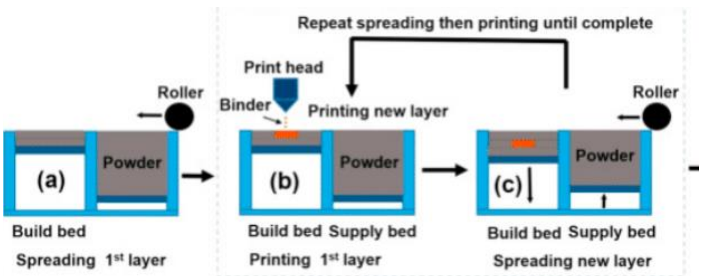

Figure 1: Conventional four step binder jet printing process [1]

As outlined in the abstract, the objective is to develop a more compact, desktop-sized binder jet printer. To achieve this, we deviate from the conventional binder jetting process by eliminating the powder bed and incorporating a powder deposition module within the gantry. This modification significantly reduces the printer's size and allows us to adapt an existing FDM printer to implement our design. The design specifications are detailed in Table 1.

Table 1: List of specifications

Need	Attribute [dimension]	Specification
Small Build Volume	Volume [cm^3]	225π cm^3
Fine detailed part	Layer Thickness [µm]	50µm
Print Stainless Steel	17-4 PH 30µm powder	Y/N
Easy to remove for sintering	Modular System	Y/N
Optimized Binder and Roller Application	Print Head Width [mm] Roller Length [cm]	50-100mm (1-2 passes) 2.5-5.0cm (1-2 passes)

Printer Design

To expedite prototype development, the team decided to integrate binder jetting technology into an existing fused deposition modeling (FDM) printer, commercially known as Solidoodle [2], as depicted in Figure 2.

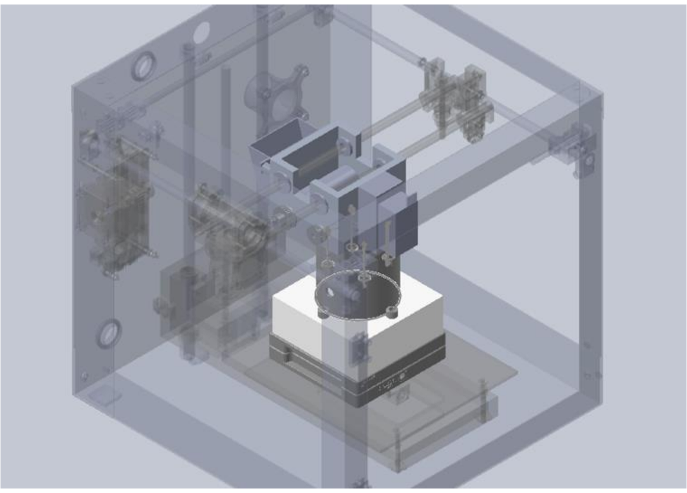

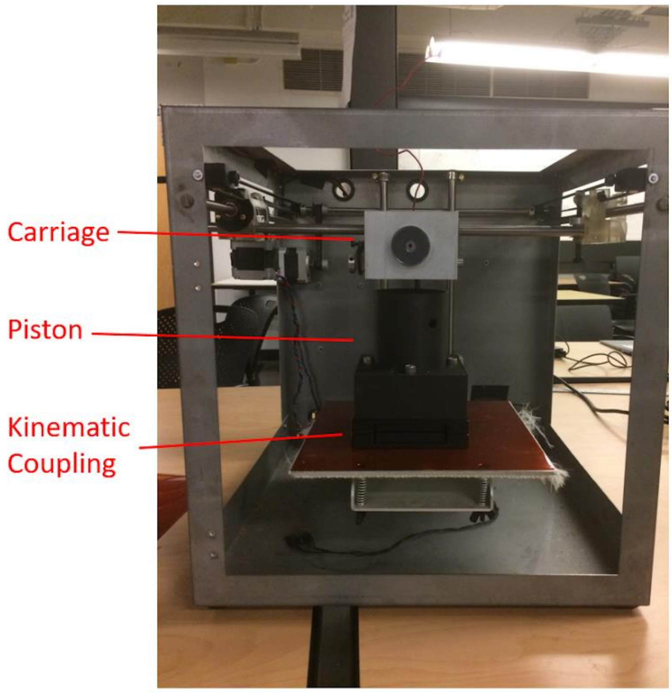

Figure 2: CAD and Prototype [2]

The binder jetting system comprises three subassemblies: carriage, piston, and kinematic coupling. These subassemblies are illustrated in Figure 3 and 4.

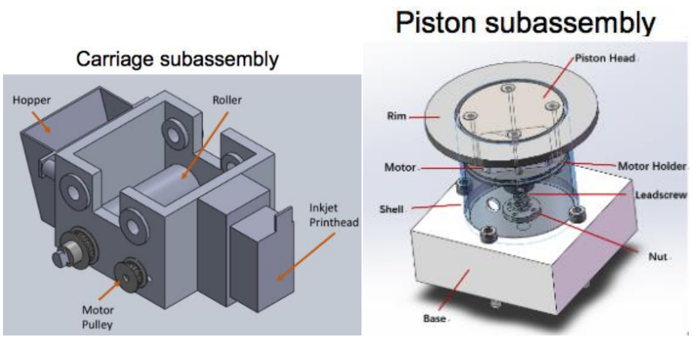

Figure 3: Carriage (Left) and Piston (Right) subassemblies

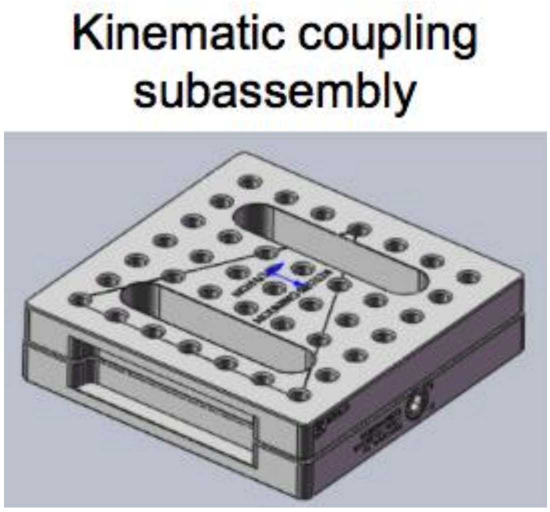

Figure 4: Kinematic coupling subassembly

Each subassembly contains additional components to provide the desired functionality. The design of the subassemblies is based on several high-level requirements, which are outlined below:

- The carriage must accommodate powder dispensing at a specified rate (this determines the hopper design, mesh size, flow rate, and vibratory motor).
- The carriage must enable powder compaction to a desired level (this specifies the roller speed, motor rating and speed, and pulley and belt dimensions).
- The carriage must support a thermal print head that dispenses binder at a particular rate with a single pass (the print head became a constraint later in the project due to limited availability of open-source printhead solutions).
- The carriage must ensure a uniform powder layer in each cycle (this sets the roller runout tolerances).
- The carriage must allow for single-pass powder dispensing and compacting (this determines the carriage width and piston diameter).
- The piston must provide precise z-axis control (this defines the lead screw diameter, pitch, and nut design).
- The design must facilitate the quick, repeatable, and precise addition and removal of the piston subassembly into the printer (this sets the selection criteria for kinematic coupling).

Print Head

(a) Printhead Selection

Print heads possess various attributes that influence their selection. Our evaluation focused on three main criteria: cost, nozzle count and configuration, and controllability, with controllability and cost being the primary considerations. Figure 5 below illustrates the trade space of different print heads based on cost and nozzle count. The optimal design, characterized by low cost and high controllability but a lower number of nozzles, was provided by Inkshield and the HP inkjet cartridge [3].

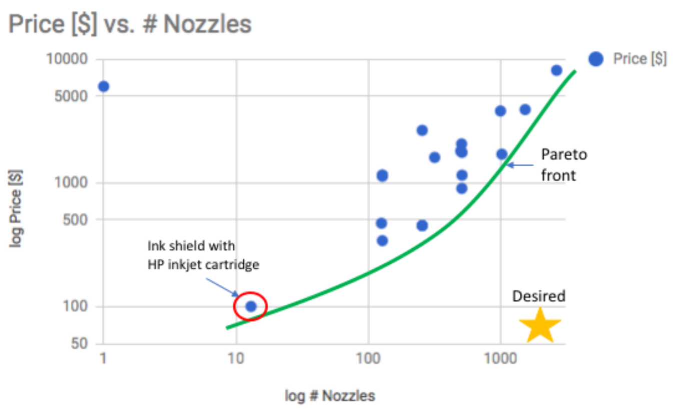

Figure 5: Printhead trade space [3]

(b) Printhead Testing

A two-axis printhead test fixture was designed to prioritize printhead testing—an inherently risky aspect of the project with numerous uncertainties—early in the design phase. This fixture assembly includes the HP printhead, an Arduino Mega, Inkshield, a base with 8mm case-hardened steel guide rods, a carriage, a piston mechanism, and digital calipers. The various components of the fixture, along with their control and resolution, are illustrated in Figure 6 below.

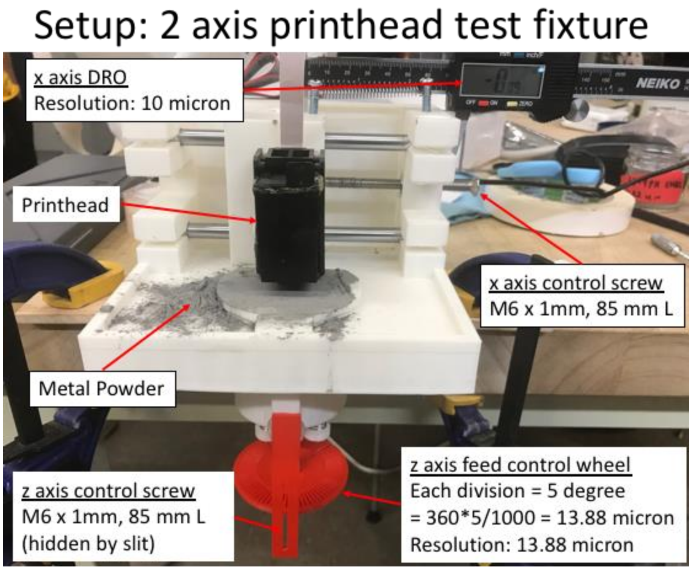

Figure 6: Printhead testing fixture

Three iterations of the piston were designed, each with different diameters, and varying groove numbers and dimensions for the gasket. Petroleum gel was used to lubricate the piston's movement within the cylinder, ensuring a proper seal. Subsequent testing showed no powder leakage.

A manually operated, 8mm diameter, case-hardened steel roller was designed to compact the powder layer for jetting. However, 0–22-micron stainless steel powder tended to adhere to the roller. Additionally, due to the fine nature of the metal powder, controlling the layer finish proved challenging. Based on these observations, further tests were conducted using coarser 14–45-micron powder.

(c) Printhead Experiments

An aqueous binder solution was prepared using one-part Acrysol WS-24 binder and five parts distilled water. The printhead was then prepped by removing the black ink, followed by cleaning and rinsing in warm water. The aqueous solution was filled into the printhead, and the jetting process was initiated using the test fixture and control electronics. Within a minute of binder jetting operation, the printhead nozzles were observed to clog. Figure 7 below illustrates the clogged nozzles and crystallized binder.

Figure 7: Clogged nozzles

It is recommended to conduct experiments with further diluted binder solutions to identify a mixture compatible with the given inkjet printhead technology. This mixture should then be tested to assess its feasibility in generating green parts and to evaluate the tolerances achievable based on various feed rates.

Chassis

The chassis, illustrated in Figure 8, fulfills three primary functions: housing the powder hopper, the roller, and the printhead. The powder hopper includes a powder holder manufactured through filament deposition modeling, a 250-micron mesh, a 14,000 RPM vibration motor, and rubber mounts to isolate vibrations from the chassis. The roller is constructed from case-hardened steel and features an 8mm shaft mounted in ball bearings. A motor drives a pulley and timing belt to counter-rotate the roller. A mount for the print head is located on the side of the chassis. The optimal spacing between the print head and the build platform is 1mm, which also determines the required positioning of the roller.

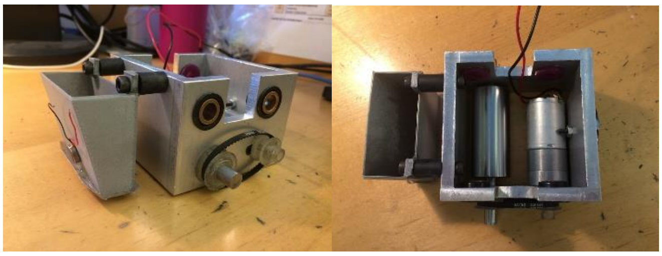

Figure 8: Chassis

(a) Powder Hopper

Qualitative experiments were conducted with the powder hopper, though quantitative experiments are a highly desirable next step. The powder used was 17-4 PH stainless steel with particle sizes of 20 microns and 30 microns. As shown in Figure 9, the 20-micron powder exhibits a cohesive texture, while the 30-micron powder has a sand-like texture. The experiments utilized the 20-micron powder based on available resources at the time.

Figure 9: 20 micron (left) vs 30 micron (right) 17-4 PH Stainless Steel Powder

A 250-micron mesh was tested with the powder, as shown in Figure 10. The mesh was selected based on the analysis of similar hopper designs and powders. The objective of this test was to confirm that the powder would only pass through the mesh when vibrated.

Figure 10: 250 Micron Mesh

Experiments were conducted with various hopper angles. Angles of 5, 10, and 15 degrees are depicted in Figure 11. However, the results indicated that the hopper angle had less impact compared to the vibration motor.

Figure 11: 5, 10, and 15-Degree Hopper Angles (left to right)

Experiments were conducted with vibration motors operating at 4300 RPM and 12000 RPM, as shown in Figure 12. The 12000 RPM vibration motor was selected for the final design due to its small coin shape, which was better suited for the intended purpose. Qualitative testing indicated that the powder dispensed much more quickly with the 12000 RPM vibration motor. One qualitative test involved operating the 12000 RPM vibration motor in intervals to control the powder flow rate. A future step with the powder hopper is to quantify the powder flow rate by weighing the deposited powder as a function of the vibration motor's operating time and characteristics.

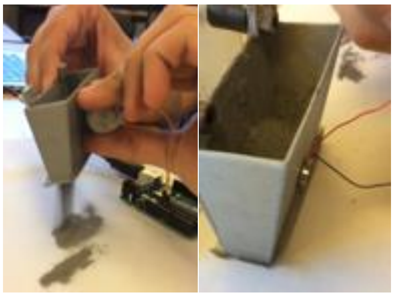

Figure 12: 4300 rpm (left) and 12000 rpm (right) Vibration Motors

(b) Roller

The precision of the roller is crucial to the chassis design, as it determines the accuracy of each powder layer. To enhance roller precision, multiple iterations of the chassis were developed.

Challenges with the initial chassis iteration stemmed primarily from the use of additively manufactured housing via stereolithography. One issue with this housing was that the holes were not precisely dimensioned, requiring post-processing such as drilling or filing. The holes in the printed part were often octagonal or similarly shaped with flat faces, influenced by the print orientation during the stereolithography process. This led to the second chassis iteration, which aimed to achieve higher precision through the use of a machined aluminum housing.

The second chassis iteration improved roller precision by employing a machined aluminum housing and an 8mm shaft within ball bearings instead of M8 screws. The precision of both the chassis and roller depended heavily on manufacturing accuracy. For instance, using a 1” collet in a lathe versus a 3-jaw chuck provided greater precision. Table 2 documents measurements of the chassis and roller, taken with a leveling gauge as shown in Figure 13. This iteration achieved a roller precision of +/- 25 microns at the roller center, reflecting the maximum precision achievable with the current design. To attain even higher precision, a new design, such as utilizing a pillow block bearing, would be necessary.

Table 2: Roller Measurements

Machine	**Tolerance offered**		
Lathe with 3 jaw chuck distance 2cm	+/- 50 microns		
Lathe with 1” collet distance 8cm	+/- 40 microns		
Lathe with 1” collet along length	+/- 5 microns		
Lathe with 1” collet distance 2cm	+/- 10 microns		
Roller in chassis	**Left end**	**Center**	**Right end**
Design Iteration #1	+/- 150 microns	+/- 75 microns	+/- 150 microns

Design Iteration #2	+/- 35 microns	+/- 25 microns	+/- 15 microns
Total improvement	**76%**	**76%**	**90%**

Figure 13: Iteration #2 Roller with Leveling Gauge

Piston and Cylinder

(a) Piston-cylinder design

The piston-cylinder assembly defines the printing volume for the workpiece. It consists of three main components: the piston sub-assembly, the cylinder, and the base. The complete assembly is depicted in Figure 14. Its dimensions are 95 x 95 x 104 mm^3.

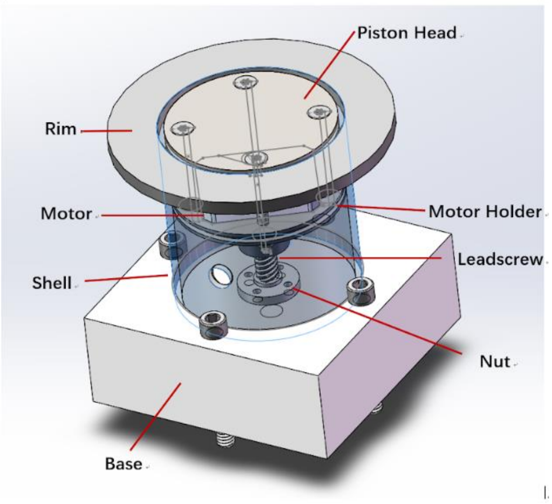

Figure 14: Components of the Piston-cylinder Assembly

Parts are printed on the piston head, which is the top of the piston subassembly. This subassembly comprises four main components: the piston head, motor holder, motor, and leadscrew. The motor is situated between the piston head and the motor holder, with its shaft coupled to a shaft-lead screw coupling. This allows it to drive an M8 x 2 mm lead screw and move the piston head along the z-axis via the coupling of the leadscrew and nut on the base.

The base, located beneath the piston subassembly and the cylinder, sits directly above the kinematic coupling. It is a 95 x 95 x 35 mm^3 block with material removed from its center to allow the lead screw to pass through the nut, which is secured to the base with four M3.5 screws. Four long ¼-20 UNC screws connect and fix the entire piston-cylinder assembly to the kinematic coupling, with a center-to-center distance of 76.2 mm (3 inches) from the center of the base. The base is designed to be as wide as possible within the 100 x 100 mm^2 dimension limit to ensure the assembly's stability, stiffness, and the piston's moving accuracy.

The cylinder encloses the piston subassembly. It is a 70mm-high tube with an inner diameter (ID) of 61.5 mm (2.42 inches) and an outer diameter (OD) of 66.3 mm (2.61 inches). A 5mm-deep indentation on the top surface of the base allows the cylinder to be bonded or press-fitted to the base.

There is a stringent dimension constraint for the design. The ID of the cylinder and the diameters of the piston head and motor holder must be at least 60 mm to accommodate the 42mm-wide square-shaped motor. The OD of the cylinder must be less than 72 mm to provide space for inserting the long screws that connect to the kinematic coupling. Finding off-the-shelf pipes or tubes within these dimensional limits is challenging. Additionally, the compact layout of components imposes higher requirements on part manufacturing and assembly, which will be discussed in a later section.

(b) Piston subassembly

The piston subassembly, depicted in Figure 15, is the sole moving component of the piston-cylinder assembly.

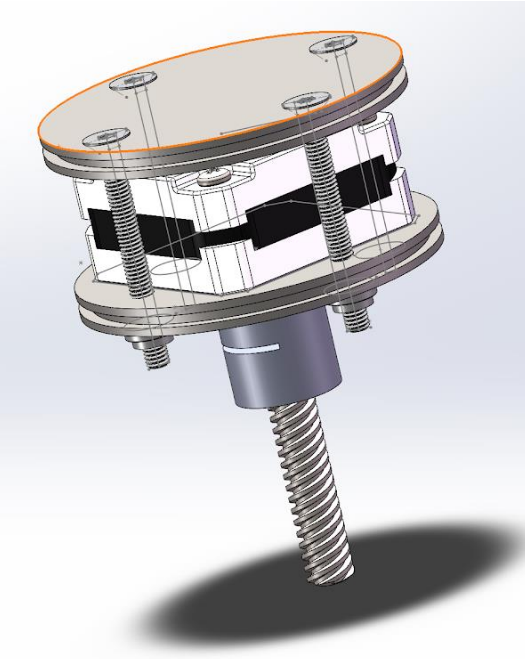

Figure 15: Piston Subassembly CAD

It consists of five parts: the piston head, motor, motor holder, coupling, and leadscrew. The motor is secured to the motor holder with four M3 screws. The piston head and motor holder are connected by four M4 screws. The layout and actual assemblies are illustrated in Figure 16 below.

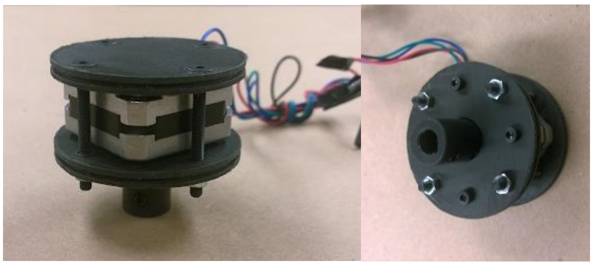

Figure 16: Real Piston Sub-assembly (Left: Top; Right: Bottom)

The NEMA 17 short-body stepper motor is used to drive the piston along the z-axis. With a thickness of 20 mm, it allows for an additional 10 mm of print height compared to the standard 40 mm-thick motor. The motor has a resolution of 1.8°, and when coupled with an M8 lead screw with a pitch of 2 mm, it achieves a z-axis resolution of 10 µm, which is ideal for the target resolution of 50 µm.

Both the piston head and motor holder are 5 mm-thick plates with a diameter of 61.5 mm (2.42 inches). These components are printed using a Markforged 2 Printer with Onyx material reinforced with chopped carbon fiber [4]. With a layer thickness of 125 µm, each part is printed in approximately 2 hours. The Onyx material offers a desirable yield strength of 470 MPa and a density of 1.3 g/cm^3, providing both strength and a favorable strength-to-weight ratio. Countersunk M4 screws are used to connect the two parts, creating a flat build area on the top surface of the piston head and preventing uneven powder packing density and its adverse effects on print quality.

(b) Cylinder subassembly

Two different cylinder sub-assemblies were fabricated: (1) Machined and (2) 3D Printed

First machined subassembly consists of two components: Aluminum (Al 6061) base and PVC cylinder as shown in Figure 17 below.

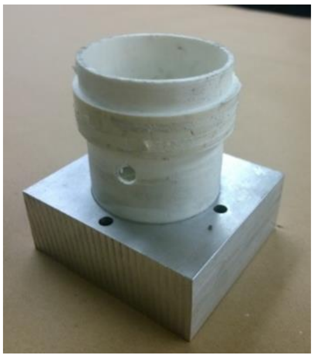

Figure 17: Machined Al base and PVC cylinder

The aluminum base, shown in Figure 18, was machined from a 1.4-inch-thick stock. A circular pocket, 2.61 inches in diameter and 0.2 inches deep, was created on the top surface of the base. Four 0.25-inch through holes were drilled around the perimeter of the circular pocket to secure it to the kinematic coupling using four M6 screws. Additionally, four 0.11-inch holes, each 0.23 inches deep, were drilled and tapped with an M3.5 x 0.6 thread tap to constrain the ball nut of the lead screw to the base.

A 0.316-inch through hole was drilled at the center of the base for the lead screw to pass through. Another concentric hole, measuring 0.40 inches in diameter and 0.39 inches deep, was drilled to position the ball nut at the center of the base, ensuring it is concentric with the lead screw.

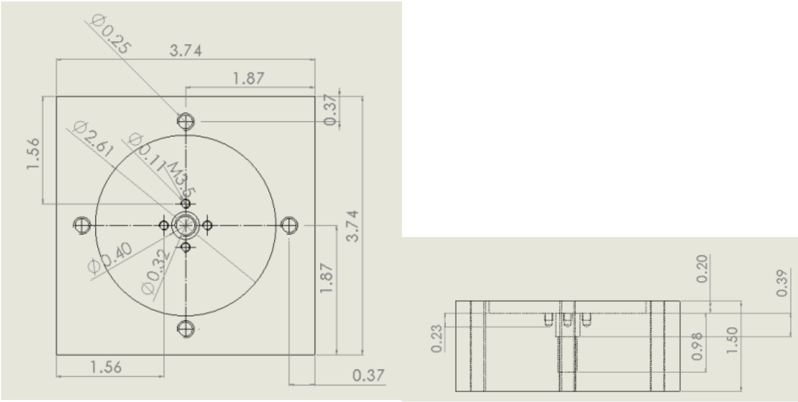

Figure 18: 2D drawing of the Al base

The cylinder was machined from a 2.9-inch PVC pipe. The pipe was cut to the required length and turned down to 2.615 inches to create an interference fit in the circular pocket of the base. A 0.5-inch diameter hole was drilled at the bottom of the cylinder to connect motor wires to the controller.

Advantages:

- Machining the aluminum base provided the high dimensional accuracy required for the powder bed mechanism. Dimensional features such as flatness, roundness, and perpendicularity were controlled as per printer requirements.
- Machining the PVC pipe for the cylinder ensured the necessary roundness, cylindricity, and parallelism.

Disadvantages:

- Designing and assembling two separate components can be challenging, particularly when high precision and tighter tolerances are required.
- Despite the high strength-to-weight ratio of Al 6061, the 1.4-inch-thick aluminum base increases the overall weight of the desktop-based binder jet printer.

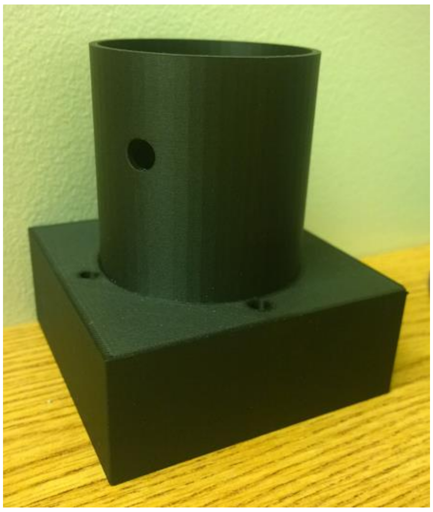

Figure 19: 3D printed cylinder sub-assembly

The second cylinder sub-assembly was printed as a single component using the Markforged Mark Two FDM 3D printer with ONYX material (nylon reinforced with carbon fiber). ONYX material is 3.5 times stiffer than standard nylon and provides better dimensional stability [4]. The carbon fibers significantly enhance heat dissipation and reduce thermal deflection, minimizing warping and enabling the printing of sharp corners. As a result, the dimensions of the part precisely matched those of the solid CAD model, as shown in Figure 19 above.

The part was printed with a triangular infill pattern, a layer thickness of 125 microns, and a fill density of 50%, optimizing both part strength and print time. Due to its geometric shape and lack of overhang features, the part was printed without any support structures, eliminating the need for post-processing. The total printing time for the cylinder sub-assembly was 30 hours.

Advantages:

- Lightweight and high strength compared to parts printed with ABS or PLA.
- Printing the cylinder and base as a single component reduced the number of assembly components from two to one.

Disadvantages:

- Dimensional accuracy and print quality of the part were limited by the printer's resolution in the X, Y (±125 microns), and Z (±100 microns) directions.
- The roundness of the cylinder was constrained by the printer's capability.

(c) Piston-Cylinder assembly

The piston-cylinder assemblies are categorized into two types based on the cylinder subassembly used: split type and single body. Both types of cylinder subassemblies were integrated with the piston subassembly to complete the piston-cylinder assembly, as illustrated in Figure 20.

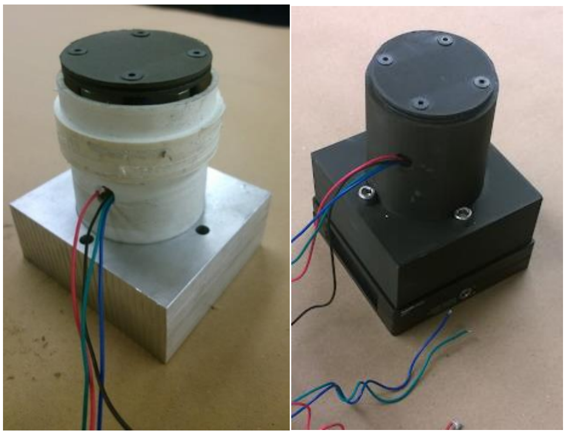

Figure 20: Split-type (left) and single (right) body assembly

The piston and cylinder were designed with a transition fit, which balances interference and clearance fits. This fit effectively constrains the piston while allowing it to move freely when actuated by the motor.

Future Work

The future scope for the piston-cylinder assembly includes the following steps:

1. Assemble the lead screw and ball nut to complete the piston assembly.
2. Test both piston-cylinder assemblies.

3. Evaluate the performance of both assemblies.

4. Integrate and test the best piston-cylinder assembly with the printer.

Conclusion

Despite encountering challenges such as printhead clogging, delayed part shipments, and incompatible controllers, the team successfully built a robust gantry system that dispenses, compacts, and binds powder to form a green part. This innovation has eliminated the need for dual piston binder jetting, allowing us to develop a more affordable and compact desktop printer. Our next steps will focus on software-level system integration, creating a controller to manage the six motors, and characterizing our printer's performance in areas such as powder flow rate, powder compatibility error, and the average part layer height. Overall, this work represents a significant first step toward future research into designing a more compact binder jetting process.

This work was supported in part by the Department of Mechanical Engineering at MIT.
Keval Babu, is a graduate student in the Department of Mechanical Engineering, Massachusetts Institute of Technology
Han He is a graduate student in the Department of Mechanical Engineering, Massachusetts Institute of Technology
Gregory Cartagena is an undergraduate student in the Department of Mechanical Engineering, Massachusetts Institute of Technology
Amardeep Sidhu is a graduate student in the Department of Engineering, Massachusetts Institute of Technology
Alison Yu is a graduate student in the Department of Mechanical Engineering, Massachusetts Institute of Technology

References

[1] Nguyen, H. X., Poudel, B., Qu, Z., Kwon, P., & Chung, H. (2024). Photopolymerization of Stainless Steel 420 Metal Suspension: Printing System and Process Development of Additive Manufacturing Technology toward High-Volume Production. *Journal of Manufacturing and Materials Processing*, *8*(5), 191. https://doi.org/10.3390/jmmp8050191

[2] Solidoodle , "Solidoodle," [Online]. Available: http://www.solidoodle.com [Accessed 15 March 2018].

[3] N.C. Lewis, "Inkshielf," [Online]. Available: http://nicholasclewis.com/projects/inkshield/ [Accessed 15 March 2018].

[4] MarkForged, " Onyx Material Datasheet Specs," [Online]. Available: https://markforged.com/materials/plastics/onyx. [Accessed 15 March 2018].